Ab-initio theoretical approach to coherent phonon generation in solids

Yasushi Shinohara[1,2], Shunsuke A. Sato[1], Kazuhiro. Yabana[1,3], Tomohito Otobe[4], Jun.-Ichi Iwata[5], George F. Bertsch[6]
[1]*Graduate School of Pure and Applied Sciences, 1-1-1 Tennoudai, University of Tsukuba, Tsukuba 305-8571, Japan*
[2]*Max-Planck Institut für Mikrostrukturphysik, Weinberg 2, D-06120, Halle, Germany*
[3]*Center for Computational Sciences, University of Tsukuba, 1-1-1 Tennoudai, Tsukuba 305-8577, Japan*
[4]*Kansai Photon Sciences Institute, Japan Atomic Energy Agency, 8-1-7 Umemidai, Kizugawa, Kyoto 619-0615, Japan*
[5]*Department of Applied Physics, University of Tokyo 70301 Hongo, Tokyo 113-8656, Japan*
[6]*Department of Physics, University of Washington, Seattle WA 98195 USA*
shinohara@nucl.ph.tsukuba.ac.jp

Abstract: We investigate mechanisms of coherent phonon generation in time-dependent density-functional theory. It provides intuitive understanding of the generation mechanism as well as its change depending on electric field frequency.
OCIS codes: (320.2250) Femtosecond phenomena; (320.7130) Ultrafast processes in condensed matter, including semiconductors

1. Introduction

We have been developing an *ab-initio* theoretical framework based on Time-Dependent Density-Functional Theory (TDDFT) to describe dynamics of electrons as well as nuclei in crystalline solids under intense and ultrashort light pulse. We have applied the framework to generation of coherent phonon to elucidate those mechanisms. In this presentation, we report our recent analysis to elucidate the mechanisms in semimetal Sb, nonpolar semiconductor Si, and polar semiconductor GaAs.

2. Theory

Our framework is capable of describing quantum dynamics of electrons and classical motion of nuclei induced by time-dependent electric field [1,2]. The electron dynamics in periodic system is described by the time-dependent Kohn-Sham equation: $i\hbar\frac{\partial}{\partial t}\psi_{nk}(\boldsymbol{r},t) = h_{KS}(\boldsymbol{r},t)\psi_{nk}(\boldsymbol{r},t)$ whose Hamiltonian has following form $h_{KS}(t) = 1/2\left(\boldsymbol{p} + e/c\,\boldsymbol{A}(t)\right)^2 + V\left(n(\boldsymbol{r},t)\right), n(\boldsymbol{r},t) = \sum_{nk}|\psi_{nk}(\boldsymbol{r},t)|^2$. We assume a spatially-uniform and time-varying electric field described by the vector potential, $\boldsymbol{\mathcal{E}}(t) = -\frac{1}{c}\frac{\partial \boldsymbol{A}}{\partial t}$ as external field. We use real-time and real-space method for the equation, introducing uniform spatial grids to express orbital function. We employ a standard approximation for the Hamiltonian in the density-functional theory: the electron-nucleus interaction represented by the norm-conserving pseudopotential and local-density approximation for the exchange-correlation potential. The nuclear motion is treated as classically, solving Newton equation, while the force is evaluated semiclassically by Eherenfest theorem: the force is calculated as Coulomb interaction between nuclear charge and expectation value of electron charge density, $M_a\frac{d^2\boldsymbol{R}_a}{dt^2} = -\sum_{nk}\left\langle\psi_{nk}(t)\left|\frac{\partial H(\boldsymbol{R}_a)}{\partial \boldsymbol{R}_a}\right|\psi_{nk}(t)\right\rangle + Z_a e\boldsymbol{\mathcal{E}}(t)$.

3. Coherent phonon generation in Sb

Sb is one of the most popular materials of coherent phonon experiment. Two Raman active modes, A_{1g} and E_g, of lattice vibration are observed as coherent phonon consistent with Raman selection rule [3]. We applied our framework to generation of Sb coherent phonon with specific polarization allowed to excite both modes [1].

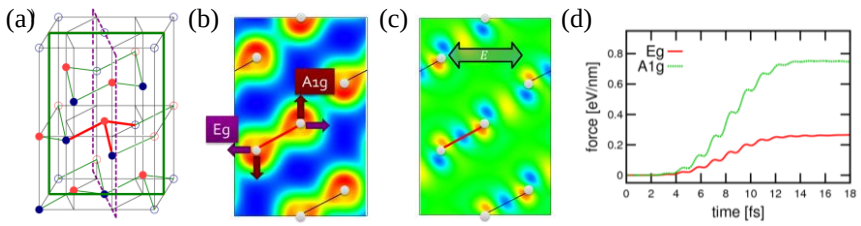

Figure 1. The panel (a) shows crystal structure of Sb for actual calculation. The red solid lines are shown to indicate bonds. The panel (b) represents electron density at ground state on the cross section enclosed by green dashed line in panel (a). The red and blue colors indicate high and low density respectively. The arrows indicate oscillation direction of both modes, A_{1g} and E_g. The panel (c) represents the density difference from one in panel (b) after laser irradiation. The red and blue colors indicate increase and decrease of electron respectively. The arrow indicates direction of polarization of electric field $\mathcal{E}$. The panel (d) shows force acting on the two lattice coordinates as a function of time. The applying electric field completely disappears after 16 fs.

The crystal structure of Sb shown in Fig. 1(a) is a super cell used in actual calculation which includes 12 Sb atoms corresponding to 6 primitive cells. Sb has three equivalent bonds as indicated as red solid lines in Fig. 1(a). One bond is on the plane expressed green solid line and other two bonds are out of the plane. At first, we perform usual density-functional calculation of ground state as initial condition of real-time dynamics. One can see high electron density around bond region in Fig. 1(b). When polarization is parallel to horizontal axis on Fig. 1(c), both A_{1g} and E_g modes should be excited according to Raman selection rule. The electron density changes permanently even after pulse irradiation due to real electron excitation caused by the applied electric field. One can see the decrease of electron density around bond region in Fig. 1(c). Such a permanent electron density decrease invokes bond elongation due to bond weakening. This is confirmed by actual calculation shown in Fig. 1(d): permanent forces acting on both coordinates appear even after pulse irradiation. The elongation direction in panel (c) includes components in two lattice coordinates, which results in appearance of forces in two lattice modes in panel (d).

4. Coherent phonon generation in Si and GaAs

Si and GaAs are also standard materials in coherent phonon measurement. Most significant difference in these two materials from Sb is the existence of band gap. The change of generation mechanism depending on photon frequency is experimentally observed in Si [4]. We investigate how the mechanism changed in bulk Si [2] and GaAs when he frequency of the applied electric field changes

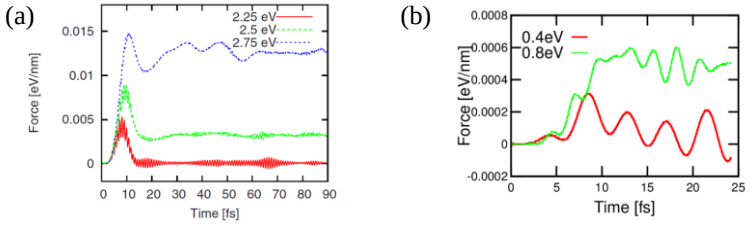

Figure 2. The panel (a) shows force acting on T_{2g} mode of Si crystal as a function of time for three laser frequencies: .2.25 eV (red solids), 2.5 eV (green dashed), 2.75 eV (blue dotted). The panel (b) shows force acting on T_{2g} mode of GaAs crystal as a function of time for two laser frequencies: 0.4 eV (red solids), 0.8 eV (green dashed). In all calculations, applied electric field is completely zero after 16 fs.

The direct band gap of Si is 2.4 eV in our calculation. Fig. 2(a) shows the forces in crystalline Si as a function of time for three laser frequencies. When the frequency is 2.75 eV which is above the gap, the force remains even after the pulse end due to real electronic excitation. This behavior is similar to that seen in Sb in which electron is really excited because of gapless system. When the frequency is 2.25 eV, namely below band gap, the force only appears while applied field exists, i.e. 0 to 16 fs. The former and latter forces account for well-known displacive and impulsive mechanisms of coherent phonon, respectively. For 2.5 eV, around the gap, the force shows a mixture of two mechanisms below and above the gap. We thus conclude that two mechanisms as well as mixture of them are included in a unified way in our framework. Fig. 2(b) shows the forces in crystalline GaAs for two laser frequencies. The direct band gap of GaAs is 0.7 eV in our calculation. The force remains even after the pulse end for 0.8 eV which is above the band gap, while average of the force after pulse end for 0.4 eV is almost zero. We thus confirm that the situation in GaAs resembles to the case of Si, although the force shown in Fig. 2(b) is still preliminary.

5. Conclusion

We presented our *ab-initio* calculation for generation of coherent phonon. For Sb, our calculation gave us intuitive understanding of generation mechanism through a change of electron density caused by the real electronic excitations. For Si and GaAs, our theoretical framework is capable of describing two mechanisms, displacive and impulsive ones, and indicates significance of the two mechanisms dependent on the laser frequency, as has been discussed in phenomenological theory.

6. References

[1] Y. Shinohara, K. Yabana, J.-I. Iwata, T. Otobe, and G.F. Bertsch, "Coherent phonon generation in time-dependent density functional theory", Phys. Rev. B 82, 155110 (2010).
[2] Y. Shinohara, S.A. Sato, K. Yabana, J.-I. Iwata, T. Otobe, and G.F. Bertsch, "Nonadiabatic generation of coherent phonons", J. Chem. Phys. 137, 22A527 (2012).
[3] K. Ishioka, M. Kitajima, and O.V. Misochko, "Coherent A_{1g} and E_g phonons of antimony", J. Appl. Phys. **103**, 123505 (2008).
[4] M. Hase, M. Kitajima, A.M. Constantinescu, and H. Petek, "The birth of a quasiparticle in silicon observed in time-frequency space", Nature **426**, 51 (2003), D.M. Riffe and A.J. Sabbah, "Coherent excitation of the optical phonon in Si: Transiently simulated Raman scattering with a finite-lifetime electronic excitation", Phys. Rev. B **76**, 085207 (2007), K. Kato, A. Ishizawa, K. Oguri, K. Tateno, T. Tawara, H. Gotoh, M. Kitajima, and H. Nakano, "Anisotropy in Ultrafast Carrier and Phonon Dynamics in p-Type Heavily Doped Si", Jpn. J. Appl. Phys. **48**, 100205 (2009).